Application of FTIR Spectroscopy and Chemometric Classification Techniques for Detecting Adulteration in Cinnamon Powder

M. Masoudi[1], R. Khodabakhshian Kargar[1*], M. R. Golzarian[1]

1- Department of Biosystems Engineering, Faculty of Agriculture, Ferdowsi University of Mashhad, Mashhad, Iran
(*- Corresponding Author Email: Khodabakhshian@um.ac.ir)
https://doi.org/10.22067/jam.2026.98580.1489

Abstract

Cinnamon is a highly valued aromatic spice widely used in the food and pharmaceutical industries. Due to its extensive applications, cinnamon is susceptible to food fraud, necessitating effective authentication methods. This study uses FTIR spectroscopy and spectral pattern analysis to establish a reliable method for detecting fraud in cinnamon powder by comparing authentic and adulterated samples. The ultimate goal is to provide a practical methodology for identifying adulteration in the spice industry. In this work, Fourier-transform infrared spectroscopy (FTIR) was employed alongside pattern recognition techniques for the authentication of cinnamon powder. To detect and classify fraudulent samples (adulterants include soybean powder, hazelnut shell powder, and dry bread powder, in different concentrations of 5%, 10% and 15% (w/w)) nondestructively, Principal Component Analysis (PCA) was utilised as an unsupervised method, while Partial Least Squares Discriminant Analysis (PLS-DA) and Soft Independent Modelling of Class Analogy (SIMCA) were applied as supervised pattern recognition approaches. The results indicated that while the spectral data of the samples were effectively classified using the PCA technique, some overlap between specific groups was noted. The overall classification accuracy achieved by the SIMCA and PLS-DA classifiers was 83% and 90%, respectively. Based on PCA modelling, SIMCA enabled the classification of samples into two distinct groups (pure vs. adulterated), and the classification accuracy of this two-class model reached 100%. These findings confirm the effectiveness of combining FTIR with pattern recognition techniques for robust and nondestructive authentication of adulterated cinnamon powder, contributing to quality control in the spice industry.

Keywords: Cinnamon authentication, Food fraud detection, Fourier-transform infrared spectroscopy, Pattern recognition techniques, Quality control in spices

Introduction

Cinnamon, derived from the inner bark of trees belonging to the genus Cinnamomum, is one of the oldest and most cherished spices globally, known for its distinctive flavour, aroma, and potential health benefits (Błaszczyk, Rosiak, & Kałużna-Czaplińska, 2021; Spence, 2023; Suriyagoda *et al.*, 2021). This spice is rich in essential oils, particularly cinnamaldehyde, which contributes to its unique taste and scent, and is packed with various bioactive compounds, including polyphenols and flavonoids, which have been linked to numerous health-promoting properties (Huang *et al.*, 2021; Zhang *et al.*, 2022). These compounds are known for their antioxidant, anti-inflammatory, and antimicrobial effects, making cinnamon not only a culinary delight but also a valuable ingredient in traditional and modern medicine (Moreno *et al.*, 2022; Pagliari *et al.*, 2023). The nutritional value of cinnamon is significant, as it contains a variety of vitamins and minerals, including calcium, manganese, and vitamin K, which can contribute to overall health when consumed as part of a balanced diet (Almatroodi *et al.*, 2020; Goel & Mishra, 2020). Given its popularity and the growing awareness of its health benefits, the demand for high-quality cinnamon powder has surged, necessitating stringent quality control measures to ensure the authenticity and purity of cinnamon products in the market (Pages-Rebull, Pérez-Ràfols, Serrano, & Díaz-Cruz, 2024).

Food fraud, particularly in spices, has emerged as a significant concern in the global food supply chain, threatening consumer

safety and confidence (Montgomery, Haughey, & Elliott, 2020; Velázquez *et al.*, 2023). The adulteration of spices, including cinnamon, is often driven by economic motives, as the high value of authentic spices creates opportunities for profit through deceptive practices (Galvin-King, 2020). Common adulteration methods include the addition of cheaper substances, such as cassia bark or artificial colouring agents, which can mislead consumers and undermine the integrity of the product (Banti, 2020; Feltes, Ballen, Steffens, Paroul, Steffens, 2023). Furthermore, the complexity of spice composition makes it challenging for consumers to identify fraud, highlighting the need for reliable detection methods. Adulteration not only affects the market but can also pose health risks to consumers, especially if harmful additives are introduced. The prevalence of such fraudulent practices calls for robust regulatory frameworks and advanced analytical techniques to safeguard consumers and maintain the quality of spice products (Vinothkanna, Dar, Liu, & Jia, 2024). Given the increasing complexity of food fraud, particularly in the spice industry, the integration of analytical techniques with legislative awareness is essential. Several studies have outlined the evolution of EU food safety legislation and its implications for quality control (Bondoc, 2016, 2015).

Several analytical techniques have been developed and employed to detect food fraud, particularly in spices like cinnamon. Traditional methods, including sensory analysis and chemical tests, often fall short in terms of specificity and reliability (Fiorino *et al.*, 2018). Recent advancements in spectroscopic methods, such as Near-Infrared Spectroscopy (NIRS), Raman Spectroscopy, and Fourier Transform Infrared (FTIR) Spectroscopy, have shown promise in providing rapid and non-destructive means of assessing the authenticity of spice products (Jiménez-Carvelo *et al.*, 2021; Kaavya *et al.*, 2020; Shawky, Nahar, Nassief, Sarker, & Ibrahim, 2024). FTIR spectroscopy, in particular, offers a unique advantage by providing detailed information about the molecular composition of samples through the analysis of vibrational transitions of molecules, allowing for the identification of specific compounds and detection of adulterants. This technique is not only effective in detecting known adulterants but can also help uncover novel fraud methods, making it a valuable tool in food safety and quality assurance (Dimitriou *et al.*, 2025; Jahan & Uddin, 2024; Querido, Kandel, & Pleshko, 2021; RP, Sankar, Sukumaran, & Savithri, 2024). Furthermore, pattern recognition methods like Principal Component Analysis (PCA), Partial Least Squares Discriminant Analysis (PLS-DA), and Soft Independent Modelling of Class Analogy (SIMCA) have been increasingly applied to interpret the spectral data, offering enhanced accuracy in distinguishing between authentic and adulterated samples (Khanban, Garmarudi, Parastar, & Toth, 2022).

In the past decade, numerous studies have focused on utilising spectroscopic techniques to detect fraud in spices, with a significant emphasis on cinnamon (Cantarelli, Moldes, Marchevsky, Azcarate, & Camiña, 2020; Castro, Ribeiro, Santos, & Páscoa, 2023; Lopes *et al.*, 2022; Sudarsh & Müller-Maatsch, 2023; Yasmin *et al.*, 2019). Research has demonstrated the effectiveness of FTIR spectroscopy in distinguishing between pure cinnamon and adulterated samples by analysing spectral patterns and identifying characteristic absorption bands associated with various components (Lixourgioti *et al.*, 2022). For instance, recent studies have successfully employed FTIR spectral analysis combined with pattern recognition techniques such as PCA, PLS-DA, and SIMCA to differentiate between Cinnamomum verum (true cinnamon) and Cinnamomum cassia (cassia), revealing distinct spectral fingerprints that can be used as a basis for authenticity testing. PCA has been widely used as an unsupervised method to reduce dimensionality and reveal patterns in the data without prior knowledge of class labels, while PLS-DA and SIMCA have been applied as supervised methods to classify and predict the authenticity of cinnamon samples

based on known categories (Hajiseyedrazi, Khorrami, & Mohammadi, 2024). These methods, combined with FTIR spectroscopy, provide a powerful framework for detecting food fraud in spices with high precision.

The primary objective of this study is to explore the application of FTIR spectroscopy for the detection of adulteration in cinnamon powder through comprehensive spectral pattern analysis. While previous studies have primarily focused on differentiating true cinnamon from cassia or identifying specific adulterants, the novelty of the present work lies in the simultaneous evaluation of three economically motivated adulterants, namely soybean powder, hazelnut shell powder, and dried bread powder, at different adulteration levels (5%, 10%, and 15% w/w). By examining the spectral characteristics of both authentic and adulterated cinnamon samples, this research aims to establish a reliable, rapid, and nondestructive methodology for identifying fraudulent practices in the spice industry. The study integrates both unsupervised and supervised chemometric techniques, including Principal Component Analysis (PCA) for exploratory analysis and dimensionality reduction, as well as Partial Least Squares Discriminant Analysis (PLS-DA) and Soft Independent Modelling of Class Analogy (SIMCA) for sample classification and authentication. Furthermore, the comparative evaluation of these classification approaches provides insights into their effectiveness for cinnamon authentication, while demonstrating the capability of SIMCA to accurately discriminate pure and adulterated samples in a binary classification framework. Through this work, we aim to contribute to food safety and quality assurance by providing a practical and cost-effective tool for routine authenticity assessment of cinnamon products, thereby strengthening consumer confidence and supporting ethical practices within the spice market.

Materials and Methods

In this study, we employed FTIR spectroscopy combined with pattern recognition techniques to develop a reliable nondestructive method for detecting adulteration in cinnamon powder. Three adulterants namely, soybean powder, hazelnut shell powder, and dry bread powder were added at concentrations of 5%, 10%, and 15% (w/w). For data analysis, we applied PCA as an unsupervised method for exploratory analysis, while PLS-DA and SIMCA were used as supervised classification approaches. The research addressed whether this approach can effectively discriminate pure from adulterated samples, with the hypothesis that significant spectral differences exist and that SIMCA can achieve high accuracy, particularly 100% in the binary pure vs. adulterated classification, whether FTIR combined with chemometrics can effectively discriminate between pure and adulterated samples across different adulterant types and concentrations (5–15% w/w), and which spectral regions are most indicative of adulteration.

Sample collection and preparation

Cinnamon sticks (*Cinnamomum verum*), soybean, hazelnut shells, and dried bread powder were sourced from local markets in Mashhad, Iran. Careful consideration was taken to ensure that each ingredient was of high quality to faithfully replicate common adulterants found in cases of food fraud. The cinnamon sticks were meticulously selected for their premium quality and prepared into cinnamon powder with a purity level of 100%. The sticks were first thoroughly cleaned to remove any surface contaminants, and then air-dried under controlled conditions to preserve their natural properties. Once fully dried, they were finely ground using a laboratory-grade grinder, producing a uniform cinnamon powder that was used as the reference for authentic samples in this study.

Laboratory-grade grinder specifications
Speed range:up to 27,000 rpm
Cup dimension:diameter 90mm,high 65mm
Cup volume: 300cc
Transperent cover
Dimensions: 220dia.x300h,8kg

For the adulterants, soybean, hazelnut shells, and powdered dried bread were prepared using established techniques documented in previous studies (Hashemi-Nasab, Talebian, & Parastar, 2023; Khodabakhshian, Bayati, & Emadi, 2021; Lixourgioti *et al.*, 2022), with minor adjustments made to suit the specific requirements of this research (Fig. 1a). Soybean grains were lightly roasted to simulate processing conditions that mimic real-world adulteration practices, and then ground into a fine powder. Hazelnut shells were thoroughly cleaned, dried at room temperature, and ground into powder form using a laboratory mill. Dried bread was ground and sieved to ensure a fine powder consistent with the texture of the other ingredients.

Laboratory- roaster specifications

Electric operation	2.4 kW
Roasting time	10-15 min
Single-phase	Voltage
Chaff recycling	Cyclone
Roasting	Hot air
Casing	Stainless steel
Noise level	50 dBA

All of the samples including cinnamon powder, soybean powder, hazelnut shell powder, and dried bread powder were partially ground for five minutes using a conventional blade grinder. This step was crucial to ensure uniform particle sizes across all samples. After grinding, a 35-mesh sieve was used, allowing both the cinnamon powder and the adulterants to pass through uniformly, ensuring consistency in particle size distribution for subsequent testing (Fig. 1b).

To create composite samples, the cinnamon powder was blended with the three adulterants at different concentration levels of 5%, 10%, and 15% (w/w) based on the weight of cinnamon powder. The adulterants were incorporated to simulate varying degrees of adulteration. The mixtures were thoroughly blended to ensure homogeneity and prevent clumping, reflecting the fraudulent practices commonly used to adulterate cinnamon powder with cheaper or more accessible materials. Each adulterated sample was carefully prepared in five replicates, including pure cinnamon powder samples as controls.

The pure cinnamon powder and each of the blended samples were stored individually in airtight plastic bags to protect them from environmental factors such as moisture and light. The storage environment was a cool, dark, and dry space, designed to prevent any degradation of the sample composition prior to spectroscopic analysis. This step was essential to maintain the integrity of the samples until testing.

Five replicates were prepared for each adulteration level (5%, 10%, and 15%), ensuring that the analysis could account for any variability in sample preparation and measurement. These replicates were used in the subsequent Fourier Transform Infrared (FTIR) spectroscopy analysis and pattern recognition techniques, including Principal Component Analysis (PCA), Partial Least Squares Discriminant Analysis (PLS-DA), and Soft Independent Modelling of Class Analogy (SIMCA), to detect and quantify the level of adulteration in the cinnamon powder (Hajiseyedrazi *et al.*, 2024).

FTIR instrument and Spectral data Measurements Signal Acquisition

Fourier Transform Infrared (FTIR) spectroscopy was employed to detect adulteration in cinnamon powder by capturing the unique molecular characteristics of both pure and adulterated samples. The spectral data were collected using an Avatar 370 FTIR spectrometer (Thermo Nicolet Corporation, Madison, WI, USA), operating within the mid-infrared range (4000–400 cm^{-1}). Equipped with a deuterated triglycine sulfate (DTGS) detector and an attenuated total reflectance (ATR) accessory, the instrument provided high sensitivity and required minimal sample preparation (Fig. 1c) (Khodabakhshian, Lavasani, & Weller, 2023). Transmittance spectra were obtained for all samples, including pure cinnamon powder and mixtures adulterated with soybean, hazelnut shells, and

dried bread powder, ensuring that the infrared light passing through the sample was recorded accurately. Each sample underwent 65 scans with a resolution of 4 cm^{-1}, and all spectra were collected in triplicate. 65 scans per spectrum were selected to achieve an optimal signal-to-noise ratio, with each of the 13 samples measured in 3–5 replicates to ensure statistical reliability. The composition of the sample groups, including pure and adulterated powders, along with the number of replicates, is summarised in Table 1. OMNIC spectroscopy software (Thermo Nicolet Corporation, Madison, WI, USA) was used to monitor and export the spectral data for subsequent analysis (Nicolau & Matzger, 2024).

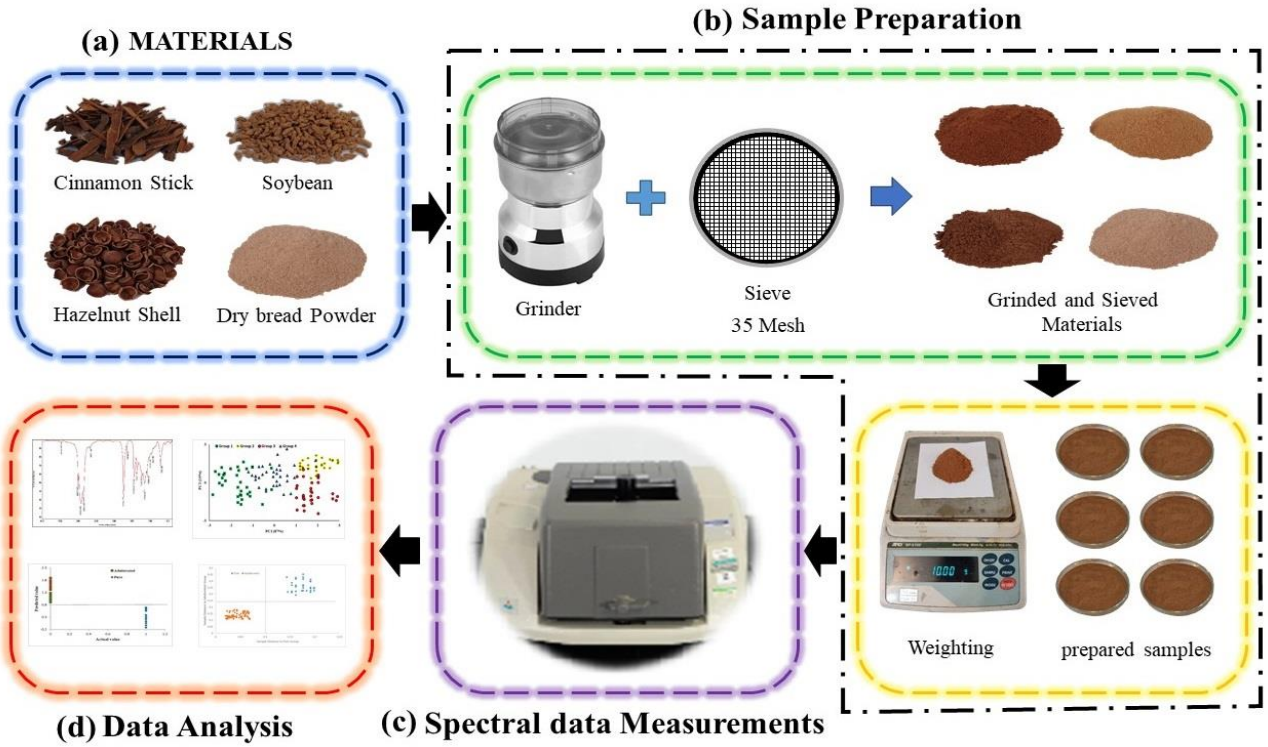

Fig. 1. Schematic diagram of the proposed procedure: (a) Base material and adulterants, (b) Sample preparation, (c) Spectral measurements, and (d) Data analysis

Table 1- Composition of sample groups and number of replicates

Sample No.	Description	Adulterant levels (% w/w)	No. of unique samples	Replicates per sample	Total measurements
1	Pure cinnamon powder	0%	1	5	5
2	Pure soybean powder	100%	1	5	5
3	Pure hazelnut shell powder	100%	1	5	5
4	Pure dried bread powder	100%	1	5	5
5	Cinnamon + Soybean powder	5%, 10%, 15%	3	5	15
6	Cinnamon + Hazelnut shell powder	5%, 10%, 15%	3	5	15
7	Cinnamon + Dried bread powder	5%, 10%, 15%	3	5	15
Total			13		65

Spectral Preprocessing

To ensure that the spectral data were accurate and free from noise or interference, several preprocessing methods were applied. Orthogonal signal correction (OSC) was used to remove extraneous variations from the data, which could otherwise mask key spectral features (Yadav, Nimi, Kapoor, & Singh, 2025). Additionally, standard normal variate transformation (SNV) and extended multiplicative scatter correction (EMSC) were utilised to correct for scattering effects caused by differences in particle size, sample thickness, or surface roughness (Wang *et al.*, 2023). These methods helped normalise the spectral data, ensuring consistency across all samples (Dashti *et al.*, 2022). Furthermore, to reduce noise and enhance peak resolution, a median filter was applied for smoothing, and Savitzky-Golay first-order (D1) and second-order (D2) derivatives were used to emphasise subtle spectral differences (Fattahi & Seyfari, 2025). Detrending was also performed to eliminate baseline drifts that could arise from environmental or instrumental factors (Wu *et al.*, 2023). To identify the most effective preprocessing approach, 18 different scenarios—including individual and combined methods (e.g., SG, SNV, MSC, OSC, SG+SNV, SG+MSC, and OSC+SG)—were evaluated. The optimal combination was selected based on model performance criteria (classification accuracy and RMSE). The final preprocessing pipeline consisted of Savitzky–Golay smoothing (second-order polynomial, 11-point window) followed by SNV, which provided the best balance between noise reduction and preservation of relevant spectral information. This approach prevented over-preprocessing and minimised the risk of losing chemically meaningful spectral features. The operations were performed using MATLAB (MathWorks Inc., Natick, MA, USA). After preprocessing, the spectra were exported to The Unscrambler software (CAMO Software, Norway), where PCA, PLS-DA, and SIMCA were applied for classification and pattern recognition analysis.

Model construction, selection of principal components / latent variables, and validation

To ensure transparent and reproducible selection of model complexity (number of principal components for SIMCA and number of latent variables for PLS-DA), we adopted the following systematic procedure. All multivariate modelling was carried out using Unscrambler® v9 (CAMO, Oslo, Norway) with the preprocessing sequence described in Section 2.2.2.

SIMCA (class-wise PCA): For each class, we constructed a class model by performing PCA on the training subset only (Cruz-Tirado *et al.*, 2023; Nargesi, Amiriparian, Bagherpour, & Kheiralipour, 2024). The optimal number of PCs for each class model was determined using 4-fold cross-validation (venetian blinds) repeated across the four random splits described in Section 3.2. Selection criteria were: (i) inspection of the PCA scree plot (cumulative explained variance and the 'elbow'), (ii) minimisation of the class prediction error (misclassification rate) under cross-validation, and (iii) stabilisation of the DModX (Distance to Model in X-space) acceptance limits (residual distance). Where the combination of criteria suggested multiple candidate PC counts, we chose the smallest number of PCs giving statistically indistinguishable classification performance (parsimony principle). The D-critical (α = 0.05) threshold was used to set SIMCA acceptance limits. The final number of PCs used for each class is reported in Table 2 and is supported by the PCA scree plots added as Figure 7.

PLS-DA (multi-class PLS2 approach): Because the problem involves more than two predefined groups (pure cinnamon and three different adulterants), we used a multivariate response PLS implementation (PLS2-DA, i.e., PLS regression with a dummy/one-hot encoded Y matrix for the classes) rather than fitting a single binary PLS-DA across all data. In practice, the Y matrix comprised four

columns (one per class) with values 1 for samples of the class and 0 for others. The PLS2 model was built in Unscrambler with the same preprocessing pipeline as the final PCA/SIMCA models. The optimal number of latent variables (LVs) was chosen by: (i) minimising the root mean squared error of cross-validation (RMSECV) in 4-fold cross-validation (the same four splits used throughout), (ii) monitoring classification accuracy and stability (sensitivity, specificity) as a function of the LV number, and (iii) avoiding overfitting by selecting the smallest LV number beyond which the RMSECV and accuracy curves plateau. RMSECV vs LV plots and classification-accuracy vs LV plots were inspected (see Figure 10). PLS-DA was performed using a one-hot encoded Y-matrix (multivariate response) for class membership, which is sometimes referred to in the literature as PLS2-DA; however, the term PLS-DA is used consistently throughout this work.

Overfitting checks and statistical significance: To confirm that the selected PLS2 models were not the result of overfitting, we performed label-permutation tests (n = 200 permutations): class labels were randomly shuffled and the PLS2 modelling procedure (including cross-validation) repeated; the distribution of accuracies obtained under label randomisation is reported in Figure 11. In addition to permutation tests, model performance is reported for calibration and external validation sets (Table 2); robustness was evaluated by repeating the random 75/25 split four times so every sample appeared once in the test sets. All final model parameters and diagnostic plots (scree plots, RMSECV curves, DModX plots, and permutation test histograms) are provided in Figures 9–11.

Unsupervised pattern recognition

Principal Component Analysis (PCA) is a widely used unsupervised machine learning technique primarily applied for dimensionality reduction and feature extraction. It transforms a high-dimensional dataset into a smaller set of orthogonal components, called principal components, which capture the most variance in the data (Barbosa, Saurina, Puignou, & Núñez, 2020). This transformation facilitates not only data compression and noise reduction but also improves model efficiency by eliminating redundant features. PCA is also instrumental in data visualisation, particularly for datasets with more than three variables. Projecting data onto the first two or three principal components enables simplified visual inspection, aiding pattern recognition and cluster analysis (Greenacre *et al.*, 2022). Moreover, by selecting the most informative components, PCA serves as an effective feature extraction method, enhancing model performance and generalisability (Akgun & Kamiloglu, 2025; Omuya, Okeyo, & Kimwele, 2021; Rana, Liaw, Lee, & Sheu, 2021).

Supervised pattern recognition

PLS-DA is a robust technique for constructing predictive models and is particularly effective in distinguishing between different classes. PLS-DA is a calibration model based on Partial Least Squares (PLS) and focuses on enhancing class separation and revealing important features in the classification data. The PLS-DA method identifies latent variables (LV) with the largest covariance with variables that indicate the sample's membership in various groups (Barbosa *et al.*, 2020; Bevilacqua *et al.*, 2013).

Soft Independent Modelling of Class Analogy (SIMCA) is a robust pattern recognition technique employed for supervised categorisation. In this method, the samples and spectra are divided into groups according to how similar they are in the principal component space. SIMCA works by building a model based on a training dataset that contains samples from different classes or categories. The method uses PCA to reduce the dimensionality of the data and identify the most important underlying factors or components. These components are then used to create a model for each class. One advantage of SIMCA is that it can handle multicollinearity issues, frequently encountered in spectroscopic data. Additionally, it offers a comprehensible visual

representation of the classification results through score plots and contribution plots, allowing for the easy interpretation of results and the identification of outliers. In essence, SIMCA is a multivariate statistical method used for classification and prediction in chemometrics. It allows for the analysis of complex spectroscopic datasets and is commonly used in the field of analytical chemistry to classify samples into different categories based on their spectral characteristics (De Angelis, Summo, Pasqualone, Faccia, & Squeo, 2024).

Classification analysis

The model's performance was assessed based on its sensitivity, precision, and specificity in detecting contamination in the cinnamon powder samples. Sensitivity indicates the percentage of correctly identified pure cinnamon powder samples in the test set. Specificity refers to the ratio of correctly detected adulterated samples to the incorrectly identified ones in the test set. These metrics were derived from the values of true positive (properly identified samples, TP), false positive (FP), true negative (TN), and false negative (incorrectly rejected samples, FN) values, as described and outlined in previous research (de Lima *et al.*, 2020).

$$Sensitivity\ (\%) = \frac{TP}{TP+FN} \times 100 \quad (1)$$

$$Specificity\ (\%) = \frac{TN}{TN+FP} \times 100 \quad (2)$$

$$Precision\ (\%) = \frac{TP}{TP+FP} \times 100 \quad (3)$$

$$Accuracy\ (\%) = \frac{TP+TN}{TP+TN+FP+FN} \times 100 \quad (4)$$

Data Splitting and Model Validation

To evaluate the performance of the classification models, the dataset was randomly divided into training and test sets using a 75/25 split ratio (75% for training and 25% for testing). To ensure the robustness and generalisability of the results, this random splitting procedure was repeated four times, and the average classification accuracy across all four runs was reported. This approach minimises the bias associated with a single random partition and provides a more reliable assessment of model performance.

Results and Discussion

Spectral analysis

Spectra of cinnamon powder, soybean powder, hazelnut shell powder, and dry bread powder are illustrated in Figs. 2, 3, 4, and 5, respectively. These figures show the IR vibrational modes of these four compounds. Experimental data are required to delineate the spectral region. In the context of characterising cinnamon powder, the fingerprint region of the IR spectra is important due to its uniqueness and distinctive peaks that signify the presence of soybean, dry bread, or hazelnut shells in cinnamon powder. The observed differences in the FTIR transmittance spectra are attributed to variations in the chemical composition and molecular structure of the samples (de Lima *et al.*, 2020).

As observed in previous studies (Boughendjioua, Amoura, & Boughendjioua, 2017; Hu, Zhang, Xiao, & Wang, 2018), the pure cinnamon spectrum exhibited characteristic absorption bands near ~1678 cm^{-1} (C=O stretching), ~1626 cm^{-1} (C=C stretching), ~1450 cm^{-1} (aromatic ring vibrations), and ~1289 cm^{-1} (O–H stretching), which are primarily associated with cinnamaldehyde, coumarin, and other phenolic compounds. In the case of dry soybean, specifically, two prominent bands near ~2924 cm^{-1} and ~2854 cm^{-1} correspond to asymmetric and symmetric stretching vibrations of aliphatic CH_2 groups in fatty acid chains, while the band near ~1745 cm^{-1} is attributed to ester carbonyl (C=O) stretching of triglycerides (Wu *et al.*, 2018), while the valley near ~1700 cm^{-1} is related to amide I and II, corresponding to protein content (Nicolaou, Xu, & Goodacre, 2010). Additionally, the amide I and II bands near ~1650 cm^{-1} and ~1540 cm^{-1}, respectively, indicate the presence of proteins. For hazelnut shells, the spectrum revealed bands characteristic of lignocellulosic materials. The peaks near ~2924 cm^{-1} and ~2845 cm^{-1} are assigned to aliphatic C–H stretching

vibrations, while the band at ~1709 cm^{-1} corresponds to carbonyl/carboxyl C=O stretching of hemicellulose and lignin. The aromatic C=C ring stretching vibrations appeared at ~1613 cm^{-1} and ~1504 cm^{-1}, and the bands at ~1370 cm^{-1}, ~1226 cm^{-1}, and ~1030 cm^{-1} are associated with aliphatic CH_3 deformation, aromatic C–O stretching, and aliphatic C–O/C–OH stretching of cellulose and hemicellulose, respectively (Özçimen & Ersoy-Meriçboyu, 2010). Also in dry bread powder, which contains wheat flour, valleys near ~1164 cm^{-1} and ~1373 cm^{-1} are attributed to ester C–H banding and sulfone, respectively. Additionally, the broad band around ~1000–1100 cm^{-1} is characteristic of glycosidic linkages in starch polymers (Dave & Modi, 2018).

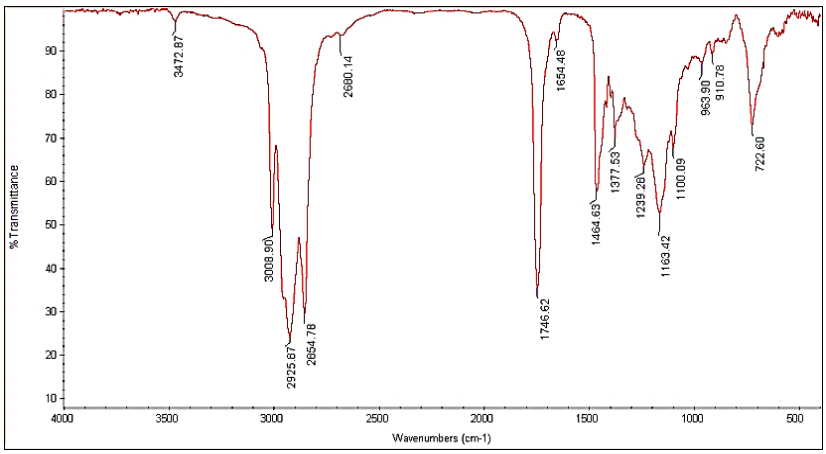

Fig. 2. FTIR spectra of pure cinnamon

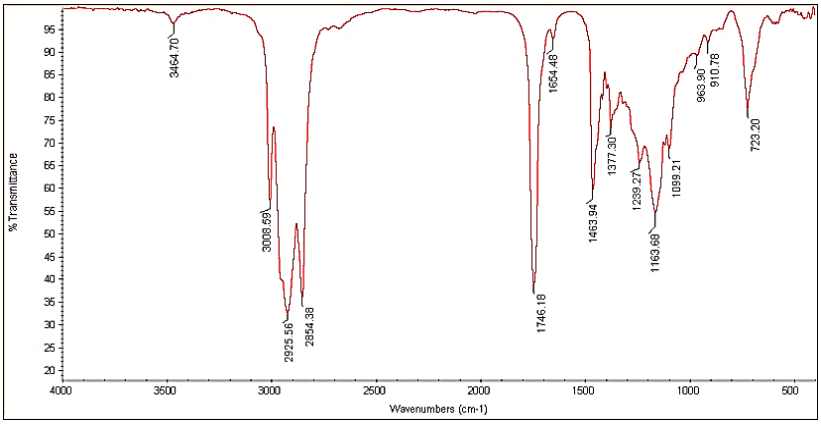

Fig. 3. FTIR spectra of dry soybean

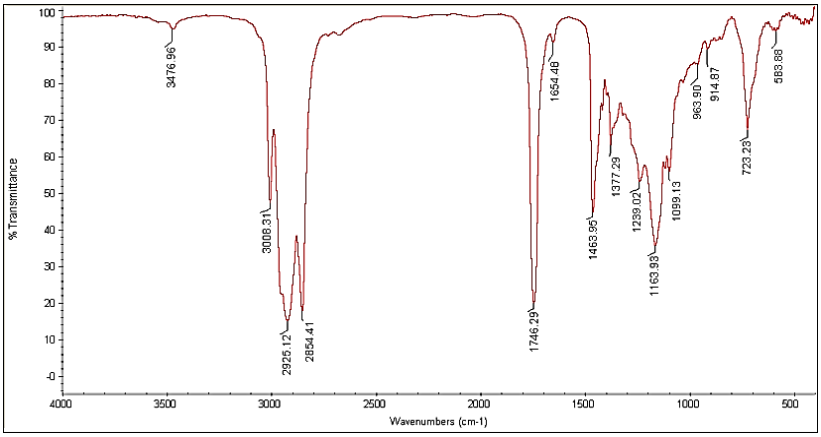

Fig. 4. FTIR spectra of hazelnut shell

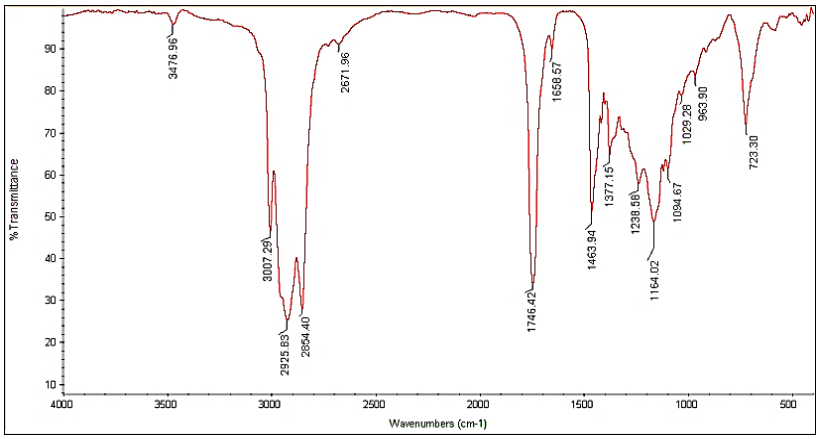

Fig. 5. FTIR spectra of dry bread

Unsupervised pattern recognition

As previously indicated, unsupervised pattern recognition aims to determine the existence of clustering in a dataset without relying on class membership information. It is advisable to initiate exploration using techniques such as PCA to describe the underlying structure of the dataset, even if the class memberships of the samples are known in advance (Khodabakhshian & Abbaspour-Fard, 2020).

The clustering of the cinnamon samples based on IR preprocessed data is shown in Figure 6, presented as a scatter plot of the PCA scores in the first two PC spaces. A PCA model comprising four principal components and ~97% explained variance was employed (PC1 = 87%, PC2 = 10%, the remaining PCs contribute the remainder). The first two PCs summarise the data in the most distinctive manner, and this plot can be used to analyse the differences and similarities among the sets of mixed samples. According to the four investigated groups, as shown in Figure 6, the distribution of data across the two PC spaces reveals scattered groupings, along with partial overlaps between certain groups, implying that spectral features of mixed samples may be similar (Figures 2–5).

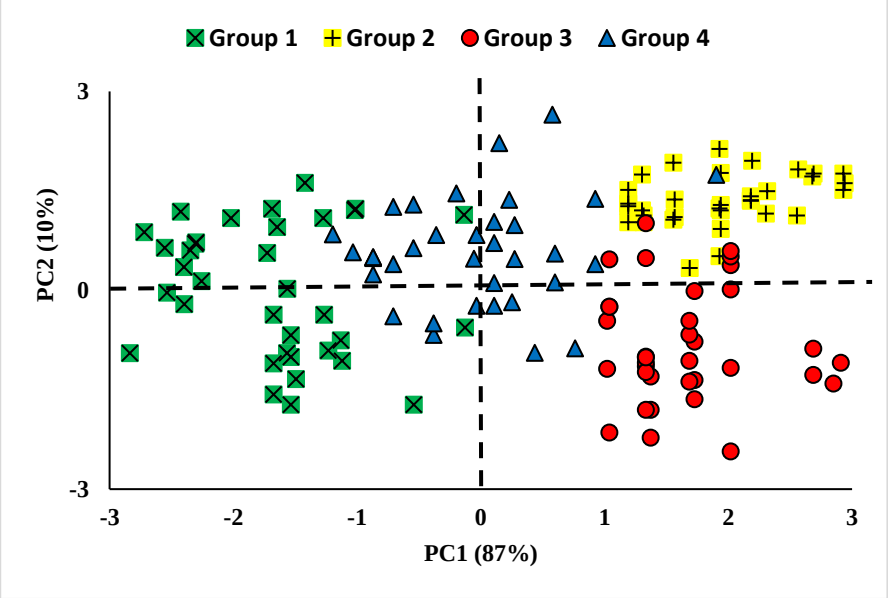

Fig. 6. Scatter plots of PCA scores in the first two principal component spaces for the clustering of the four studied mixture samples: "Group 1: pure cinnamon", "Group 2: cinnamon + soybean", "Group 3: cinnamon + hazelnut shell", and "Group 4: cinnamon + bread powder"

To identify the spectral variables responsible for the separation observed in the PCA score plot, the loading plots of the first two principal components were examined (Figure 7). The loading profiles indicate that discrimination between pure and adulterated cinnamon samples is mainly governed by absorption bands located within the fingerprint region together with several characteristic functional-group vibrations. The highest absolute loading values were observed around 2924–2854 cm^{-1}, corresponding to aliphatic CH_2 stretching vibrations mainly associated with lipids in soybean powder, around 1700–1650 cm^{-1} related to carbonyl stretching and amide I vibrations, near 1600–1500 cm^{-1} attributed to aromatic C=C skeletal vibrations of lignin and phenolic compounds, and within 1200–1000 cm^{-1} corresponding to C–O–C and C–O stretching vibrations of carbohydrates and polysaccharides. These spectral regions therefore contributed most strongly to the separation of pure cinnamon from samples adulterated with soybean powder, hazelnut shell powder, and dried bread powder.

However, PCA is an unsupervised decomposition of spectral variance and the largest variance directions (PC1, PC2) need not contain all the subtle but class-discriminant information required for robust supervised classification. In particular, inter-class differences related to minor spectral features (e.g., subtle absorbances introduced by specific adulterant composition and interaction effects at low adulteration levels) can be captured by higher-order PCs that explain only a small fraction of total variance but nonetheless carry important discriminative information for class modelling. To determine the number of PCs used in each SIMCA class model, we therefore examined: (i) the PCA scree plots (variance explained vs PC number), (ii) the cross-validated class prediction error as a function of the number of PCs, and (iii) the DModX residuals and acceptance limits. The scree plots (Figure 8) show a pronounced 'elbow', but inspection of class-wise prediction error under 4-fold cross-validation (repeated across four random splits) indicated that inclusion of PCs up to the 4th (and PC5 for Group 1) produced small but consistent improvements in sensitivity for the class models and reduced misclassification of borderline samples.

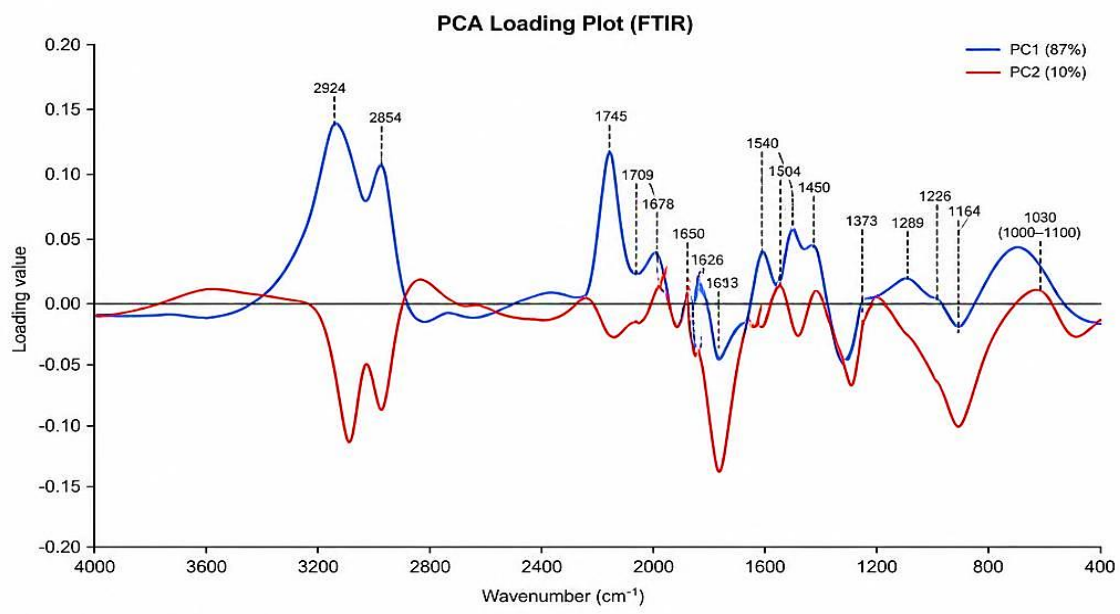

Interpretation of Loading Peaks

Wavenumber (cm⁻¹)	Assignment	Origin / Chemical Assignment
2924	CH_2 asymmetric stretching	Lipids (soybean triglycerides)
2854	CH_2 symmetric stretching	Lipids (soybean triglycerides)
1745	Ester C=O stretching	Triglycerides (soybean, bread lipids) Hemicellulose acetyl/uronic esters
1709	Carboxylic acid C=O	Phenolic acids, oxidized lipids
1678	Amide I (C=O stretching)	Proteins (soybean)
1650	Amide I / Conjugated C=O	Proteins (soybean) Conjugated carbonyls, lignin

Wavenumber (cm⁻¹)	Assignment	Origin / Chemical Assignment
1626	Aromatic C=C stretching	Phenolics, lignin (cinnamon, hazelnut shell)
1613	Aromatic ring vibration	Phenolics, lignin
1540	Amide II (N–H bending)	Proteins (soybean)
1504	Aromatic C=C stretching	Phenolics, lignin (cinnamon, hazelnut shell)
1450	Aromatic ring vibration / CH_2 bend	Cinnamon (cinnamaldehyde), lignin
1373	CH bending (C–H)	Carbohydrates (bread starch)
1289	C–O stretching (phenolic)	Phenolics, lignin
1226	Aromatic C–O stretching	Lignin (hazelnut shell)
1164	C–O–C / C–O stretching	Esters, hemicellulose (bread)
1030–1000	C–O stretching	Cellulose, hemicellulose, starch (bread), polysaccharides

Fig. 7. PCA loading plots of PC1 and PC2 derived from the FTIR spectra of pure and adulterated cinnamon powders. The loading profiles identify the wavenumbers contributing most strongly to sample discrimination. Positive and negative loading peaks indicate spectral regions responsible for the separation observed in the PCA score plot

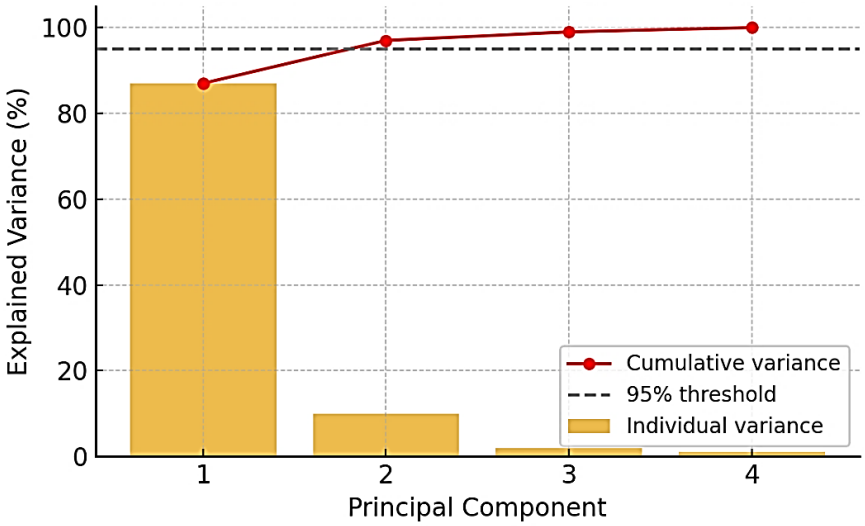

Fig. 8. Scree plot of the PCA model applied to the FTIR spectra of cinnamon and adulterated samples. Individual variance explained by each principal component (bars) and cumulative variance (red line) are shown. The ‘elbow’ at the 4th PC indicates the optimal number of PCs for SIMCA modelling of Groups 2–4, while Group 1 requires 5 PCs

Therefore, to balance parsimony and predictive performance, we selected 4 PCs for Groups 2–4 and 5 PCs for Group 1 (Table 2). The SIMCA decision boundaries and DModX plots are included in Figure 9 to demonstrate how the acceptance limits were set. Due to the observed overlaps in unsupervised clustering, two robust classifiers (PLS-DA and SIMCA) were further employed as supervised pattern recognition algorithms to enhance differentiation. The data analysis also showed that IR spectroscopy can be effectively applied to supervised classification, distinguishing between pure and adulterated samples and categorising them based on spectral characteristics.

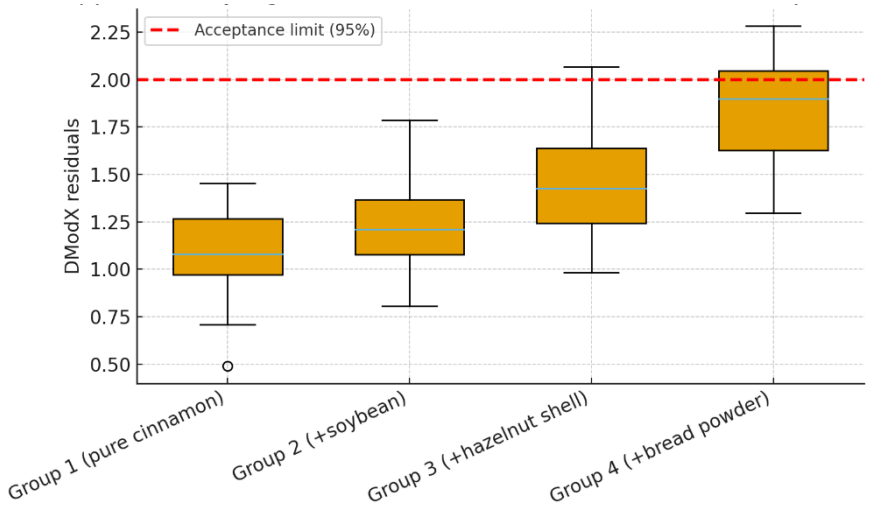

Fig. 9. DModX residuals for each SIMCA class model, showing the distribution of residuals for Groups 1–4. The red dashed line indicates the acceptance limit (95% confidence), demonstrating that all samples fall within the model boundaries and justifying the selected number of PCs for each group

Supervised pattern recognition

SIMCA and PLS-DA, as supervised classification algorithms, were applied to the IR spectra based on the findings from the unsupervised method described in Materials and Methods. These algorithms develop classification rules using a training dataset to predict the class of unknown samples. In the training phase, 75% of the samples were randomly assigned to the training set, and the remaining 25% to the test set. This process was repeated four times to ensure that each sample was included in the test set once. The reported results represent the average of these iterations. Model performance was evaluated using prediction accuracy, defined as the percentage of test samples correctly classified based on the rules established during training. SIMCA and PLS-DA models were assessed in terms of sensitivity, precision, and specificity for both calibration and validation datasets, as presented in Table 2. The optimal number of principal components (PCs) for SIMCA was found to be 4 or 5. The validation samples were then classified using the respective PCA models. For supervised classification, a multi-response PLS implementation (PLS2-DA) was used, in which class membership was encoded as a one-hot (dummy) Y matrix with four columns, one per class. This approach allows simultaneous modelling of all four classes within a single multivariate regression framework and is the appropriate extension of binary PLS-DA when multiple classes are present.

Table 2- Calibration and validation results of PLS-DA and SIMCA in terms of sensitivity, precision, and specificity (percentage) for authentication of cinnamon samples

Method	Group	No. of PC / LV	Evaluation	Sensitivity	Specificity	Precision	Accuracy
SIMCA	Group 1	5 PCs	Calibration	0.93	0.42	0.78	
			Validation	0.91	0.41	0.77	
	Group 2	4 PCs	Calibration	0.88	0.74	0.91	
			Validation	0.87	0.76	0.90	
	Group 3	4 PCs	Calibration	0.85	0.76	0.81	
			Validation	0.84	0.75	0.80	
	Group 4	4 PCs	Calibration	0.90	0.77	0.89	
			Validation	0.89	0.76	0.86	
Overall			Calibration	–	–	–	0.85
			Validation	–	–	–	0.83
PLS-DA	Group 1	9 LVs	Calibration	0.82	0.94	0.92	
			Validation	0.80	0.92	0.91	
	Group 2	8 LVs	Calibration	0.77	0.92	0.90	
			Validation	0.78	0.92	0.89	
	Group 3	8 LVs	Calibration	0.79	0.93	0.91	
			Validation	0.77	0.92	0.88	
	Group 4	9 LVs	Calibration	0.80	0.91	0.90	
			Validation	0.78	0.90	0.89	
Overall			Calibration	–	–	–	0.91
			Validation	–	–	–	0.90

The number of latent variables (LVs) for each PLS2-DA model was selected using the same 4-fold cross-validation scheme used throughout the study (each of the four random splits described in Section 2.4.3). RMSECV (root mean squared error of cross-validation) vs number of LVs was plotted, and validation classification accuracy (sensitivity/specificity/precision) was monitored as a function of LV count. The RMSECV and accuracy curves (Figure 10) show that model performance improves with increasing LV numbers up to a plateau: beyond 8–9 LVs, there is no further reduction in RMSECV nor appreciable gain in classification accuracy, while model complexity increases. Thus, the LV choice of 8–9 represents the point at which adding additional LVs fails to provide meaningful improvement (standard bias-variance tradeoff). The final LV counts used for each class are reported in Table 2.

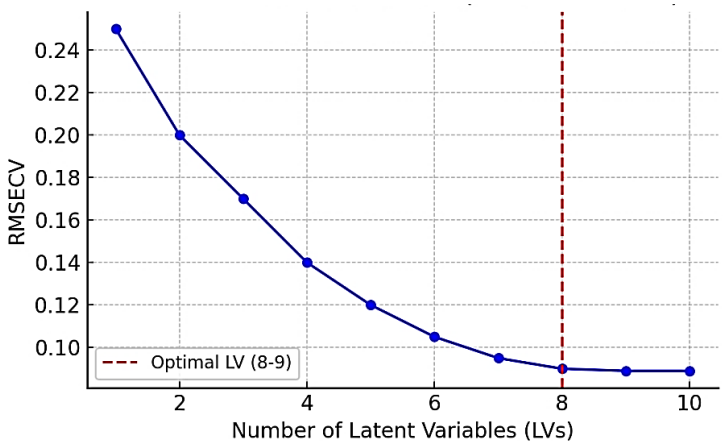

Fig. 10. Root mean square error of cross-validation (RMSECV) as a function of the number of latent variables (LVs) for PLS-DA classification of the four cinnamon sample groups. The minimum RMSECV at 8–9 LVs indicates the optimal model complexity for robust discrimination

To assess whether the relatively higher LV counts reflected overfitting, a label-permutation test (200 permutations) was performed: the distribution of classification accuracies under randomly permuted class labels is shown in Figure 11. The observed model accuracies for correctly labelled data lie well outside the permutation distribution, confirming that the chosen PLS2-DA models capture genuine class structure rather than fitting random noise. Moreover, the cross-validation procedure was repeated across four different random 75/25 splits (so that each sample was used once in test sets), and the reported calibration and validation performance values in Table 2 are averages over these repeats.

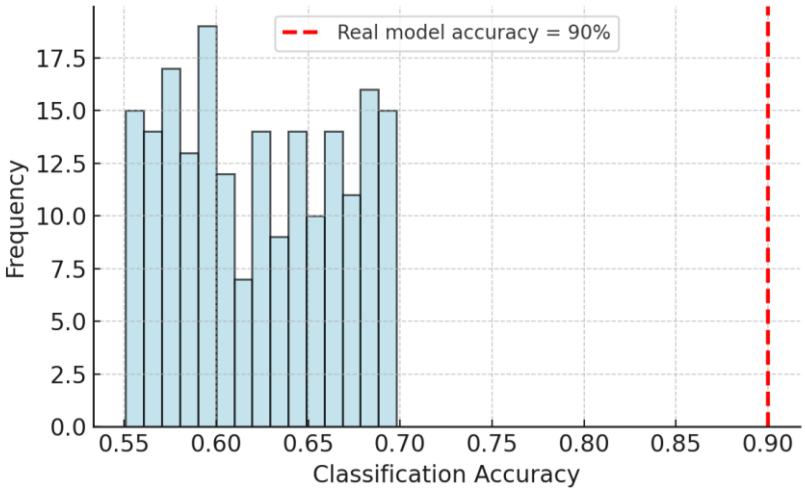

Fig. 11. Permutation test for PLS-DA classification of the cinnamon samples. Histogram represents the distribution of classification accuracies for 200 randomly permuted models, while the red dashed line shows the accuracy of the actual PLS-DA model (90%), confirming model validity and absence of overfitting

Table 2 presents calibration and validation results for both SIMCA and PLS-DA, showing sensitivity, precision, and specificity percentages for cinnamon sample authentication. For instance, SIMCA's precision for group 1 was the lowest (77%) due to overlap with other groups, particularly group 4 (Fig. 6). Four samples from group 1 were misclassified as group 4. This suggests that SIMCA, which relies on PCA modelling, performs less effectively when distinguishing between pure cinnamon and samples with different adulterants. In contrast, group 2 samples (cinnamon mixed with soybean powder) were correctly classified with 90% precision. Overall, SIMCA's classification precision across the four groups was 83%. This poor performance can be attributed to significant spectral overlaps among the different adulterant classes, as also observed in the PCA score plots. These overlaps make it difficult for SIMCA to distinguish between individual adulterant types, especially at lower concentrations. However, when the model was simplified to a binary classification problem (pure vs. adulterated), the spectral differences became more pronounced, and the two-class SIMCA model achieved 100% classification accuracy (as presented in Table 3). Due to this limitation, SIMCA was also applied to a simplified two-class problem: pure (group 1) vs. adulterated (groups 2, 3, and 4). In this case, 75% of samples were used for calibration and 25% for validation. The model achieved 100% precision for both sets, as shown in Table 3. For the two-class analysis presented in Table 3, all adulterated samples, regardless of adulterant type or concentration were merged into a single 'adulterated' class, while pure cinnamon samples formed the second

class. This binary classification was performed on the same dataset used for the four-class analysis.

As mentioned, the overall classification accuracy of the SIMCA model for the 4-class classification (pure, soybean-adulterated, hazelnut shell-adulterated, and dry bread-adulterated) was 83%, which is considerably lower than the 100% accuracy achieved in the binary (pure vs. adulterated) classification. This discrepancy can be attributed to the spectral similarities among certain adulterants. In particular, dry bread powder and hazelnut shell powder share common lignocellulosic and carbohydrate components, resulting in significant spectral overlap in the region of 1500–800 cm^{-1}. Both materials exhibit absorption bands related to C–O–C stretching (around 1000–1100 cm^{-1}), C–H bending (~1370 cm^{-1}), and aromatic C=C vibrations (~1600 cm^{-1}), which make their differentiation challenging. In contrast, soybean powder contains higher amounts of lipids and proteins, with distinct bands near 2924 cm^{-1} and 2854 cm^{-1} (CH_2 stretching) and 1650 cm^{-1} and 1540 cm^{-1} (amide I and II), providing more discriminative spectral features. These findings indicate that while SIMCA is highly effective for binary authentication (detecting the presence of any adulterant), its performance decreases when distinguishing between adulterants with similar botanical origins or chemical compositions. This highlights the need for complementary analytical techniques or higher-resolution spectral data for fine-grained adulterant identification.

Table 3- SIMCA grouping results of calibration and validation for discrimination of samples into pure and adulterated groups

Method	Group	No. of PC	Calibration set Correctly classified (%)	Validation set Correctly classified (%)
SIMCA	Pure	4	100	100
	Adulterated	4	100	100
	Overall		100	100

Figure 12 shows PLS-DA calibration results, with a cutoff value of 0.8: samples with predicted values above 0.8 were labelled as adulterated; otherwise, they were considered pure. Coomans' plots (Figure 14) were used to visually assess classification results. These plots represent the orthogonal distances between projected patterns in PCA space. The distance helps distinguish between pure and adulterated samples based on spectral features. Samples not conforming to the pure group fall below a horizontal membership limit, indicating insufficient similarity. Thus, PCA-based SIMCA effectively differentiated pure from adulterated cinnamon powders in the 400–4000 cm^{-1} spectral range.

The PLS-DA loading plot (Figure 13) confirms the importance of the same spectral regions identified by PCA. The variables located near 2924–2854 cm^{-1}, 1700–1600 cm^{-1}, and 1200–1000 cm^{-1} exhibited the largest absolute coefficients, indicating that these bands provide the greatest discriminatory power for classification. The coincidence between PCA loadings and PLS-DA coefficients demonstrates that the observed discrimination is chemically meaningful rather than resulting from statistical artefacts.

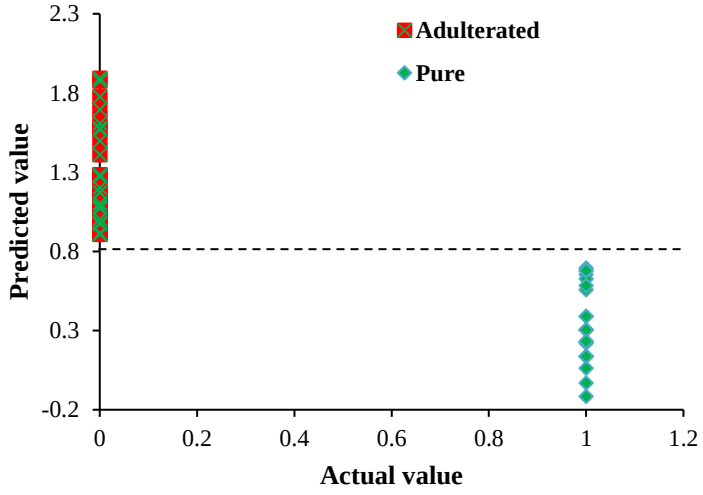

Fig. 12. The PLS-DA grouping results of the test sample sets

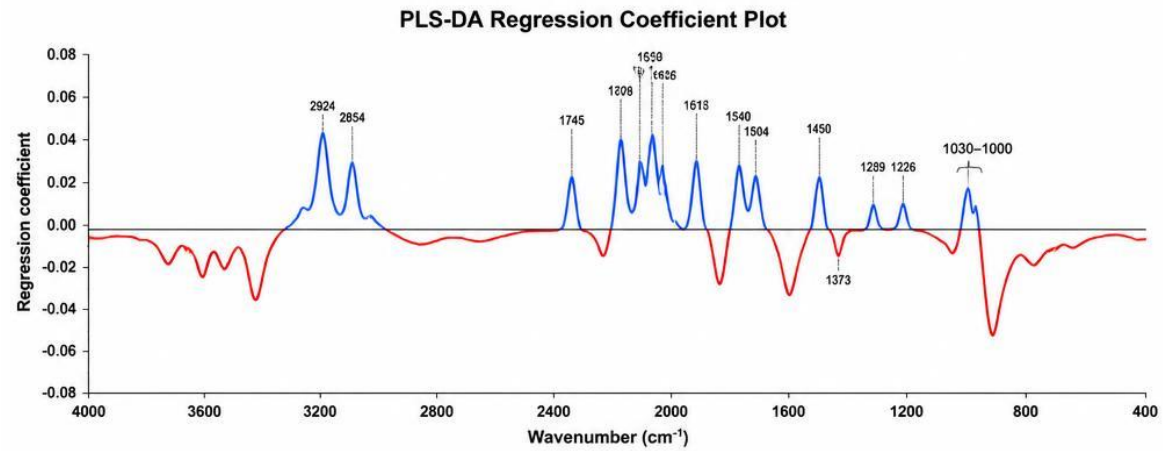

Fig. 13. PLS-DA regression coefficient (loading) plot showing the contribution of FTIR variables to the discrimination of pure and adulterated cinnamon samples. Peaks with large absolute coefficient values represent the most influential spectral regions for classification

According to Table 2, the optimal number of latent variables (LVs) for the PLS-DA models ranged from 8 to 9, depending on the group. Although this may appear relatively high, it is justified based on the complexity of the dataset and the need to capture subtle spectral differences among the classes. The full dataset comprised a total of 65 samples, with 75% used for model calibration and 25% used for validation in each iteration. Additionally, a four-fold cross-validation procedure was employed to reduce the risk of overfitting and ensure model generalisability. Despite the relatively high number of LVs, the stability of validation results and the high classification accuracy indicate that the models remained robust and were not overfitted.

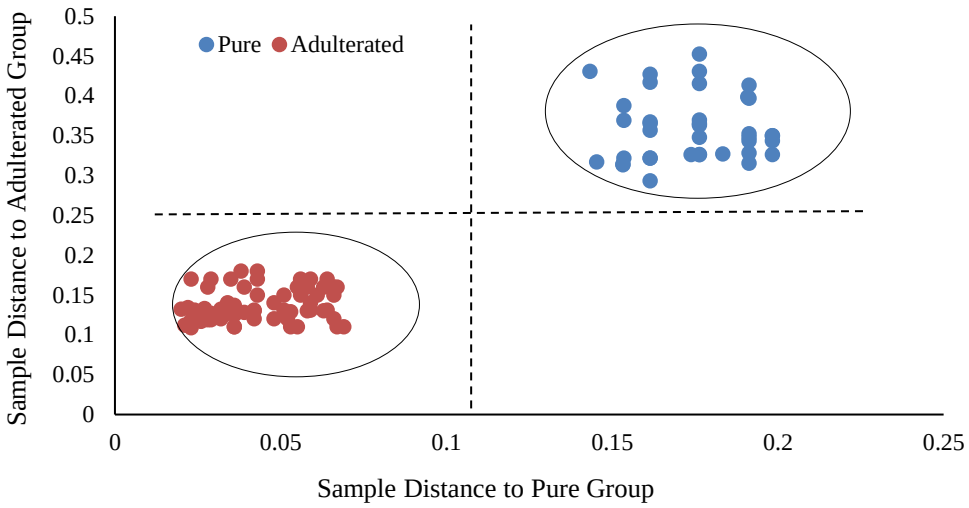

Fig. 14. The Coomans' plot of the test sample sets of pure and adulterated cinnamon groups

Overall, PLS-DA achieved 91% and 90% accuracy for calibration and validation sets, respectively, and outperformed SIMCA in classifying the four groups. Unlike SIMCA, which builds individual PCA models for each group based solely on spectral information, PLS-DA extracts relevant spectral features that maximise separation among groups. This gives PLS-DA a performance advantage. Previous studies have shown similar applications of PLS-DA in classifying agricultural products such as pomegranate (Khodabakhshian & Abbaspour-Fard, 2020), turmeric (Khodabakhshian *et al.*, 2021), black pepper and cumin (de Lima *et al.*, 2020), and cinnamon (Lixourgioti *et al.*, 2022).

Taken together, the RMSECV curves (Figure 10), the scree plots for SIMCA (Figure 8), the DModX diagnostics (Figure 9), and the permutation tests (Figure 10) provide a comprehensive, data-driven justification for the chosen model complexities: 4–5 PCs for SIMCA class models and 8–9 LVs for PLS2-DA.

Finally, a high explained variance in the first two PCs does not obviate the need for additional model components in supervised methods. PCA and supervised PLS/PCA-based classifiers have different objectives: PCA describes dominant sources of variance, while supervised methods seek to maximise class-relevant covariance. The complementary use of both approaches, unsupervised PCA to explore data structure and supervised PLS2-DA/SIMCA with explicit cross-validation and diagnostic checks, yields a robust classification suitable for the subtle discrimination tasks encountered in this study.

Conclusion

This study investigated the potential of using Fourier Transform Infrared (FTIR) spectroscopy, in combination with pattern recognition techniques namely, Principal Component Analysis (PCA), Partial Least Squares Discriminant Analysis (PLS-DA), and Soft Independent Modelling of Class Analogy (SIMCA) to detect adulteration in cinnamon powder samples within the 400–4000 cm^{-1} wavenumber range. Both pure and adulterated samples (comprising cinnamon powder mixed with soybean powder, hazelnut shell powder, and dry bread powder) were analysed through their FTIR spectra, revealing distinct molecular signatures for each sample. The study demonstrated the effectiveness of supervised pattern recognition methods, where PLS-DA achieved a high precision rate of 90%

in discriminating between pure and adulterated samples. SIMCA, though slightly less precise, still managed an impressive precision of 83%. Also, it should be noted that the two-class SIMCA model (pure vs. adulterated) achieved 100% classification accuracy, as presented in Table 3, confirming its effectiveness as a binary screening tool for detecting adulteration in cinnamon powder. Despite some overlap between certain groups, particularly at lower adulteration levels, the data distribution across the two principal component spaces clearly exhibited distinct clusters corresponding to adulterated groups. When grouping the samples into two broad categories of pure and adulterated, an acceptable level of separation was observed, with both PLS-DA and SIMCA effectively distinguishing the samples. SIMCA, while achieving 83% precision in overall group discrimination, was highly effective in classifying pure and adulterated samples. This study highlights FTIR spectroscopy, combined with these multivariate analysis techniques, as a powerful tool for rapid, nondestructive detection of adulteration in cinnamon powder. Given the accuracy achieved, this approach offers a reliable and efficient method for identifying food fraud. Future research could extend these findings to other spice powders, further solidifying the role of FTIR and pattern recognition in food quality assurance.

Acknowledgement

The authors would like to thank Ferdowsi University of Mashhad for providing the laboratory facilities and financial support.

Author Contributions

Mohammad Masoudi: Conceptualisation, Methodology, Data acquisition, Visualisation, Review and editing services, Draft.

Rasool Khodabakhshian Kargar: Supervision, Conceptualisation, Methodology, Data pre- and post-processing, Statistical analysis, Review and editing services, Draft.

Mahmood Reza Golzarian: Review and editing services, Validation, Draft.

References

1. Akgun, B., & Kamiloglu, S. (2025). Methods of cinnamon analysis. In M. F. Ramadan & M. A. Farag (Eds.), *Cinnamon: Production, processing, and functional properties* (pp. 201–217). Academic Press. https://doi.org/10.1016/B978-0-443-21820-0.00014-3
2. Almatroodi, S. A., Alsahli, M. A., Almatroudi, A., Anwar, S., Verma, A. K., Dev, K., Rahmani, & A. H. (2020). Cinnamon and its active compounds: A potential candidate in disease and tumour management through modulating various genes activity. *Gene Reports, 21*, 100966. https://doi.org/10.1016/j.genrep.2020.100966
3. Banti, M. (2020). Food adulteration and some methods of detection, review. *International Journal of Nutrition and Food Sciences*, 9, 86-94. https://doi.org/10.11648/j.ijnfs.20200903.13
4. Barbosa, S., Saurina, J., Puignou, L., & Núñez, O. (2020). Classification and authentication of paprika by UHPLC-HRMS fingerprinting and multivariate calibration methods (PCA and PLS-DA). *Foods, 9*, 486. https://doi.org/10.3390/foods9040486
5. Bevilacqua, M., Bucci, R., Magrì, A. D., Magrì, A. L., Nescatelli, R., & Marini, F. (2013). Classification and class-modelling. In F. Marini (Ed.), *Chemometrics in food chemistry* (Data Handling in Science and Technology, Vol. 28, pp. 171–233). Amsterdam, Netherlands: Elsevier. https://doi.org/10.1016/B978-0-444-59528-7.00005-3
6. Błaszczyk, N., Rosiak, A., & Kałużna-Czaplińska, J. (2021). The potential role of cinnamon in human health. *Forests, 12*, 648. https://doi.org/10.3390/f12050648
7. Bondoc, I. (2016). European regulation in the veterinary sanitary and food safety area, a component of the European policies on the safety of food products and the protection of consumer interests: A 2007 retrospective. Part two: Regulations. *Universul Juridic, Supliment*, 16-19.

8. Bondoc, I. (2015). *Foundations of veterinary sanitary and food safety legislation* (Treatise, 1st ed., Vol. 1). Iași, Romania: Ion Ionescu de la Brad Publishing House.
9. Boughendjioua, H., Amoura, N., & Boughendjioua, Z. (2017). Purity specifications of constituents of cinnamon essential oil by Fourier transformed infrared spectroscopy analysis. *Indian Journal of Pharmaceutical and Biological Research, 5*(2), 36-40. https://doi.org/10.30750/ijpbr.5.2.7
10. Cantarelli, M. Á., Moldes, C. A., Marchevsky, E. J., Azcarate, S. M., & Camiña, J. M. (2020). Low-cost analytic method for the identification of Cinnamon adulteration. *Microchemical Journal*, *159*, 105513. https://doi.org/10.1016/j.microc.2020.105513
11. Castro, R. C., Ribeiro, D. S. M., Santos, J. L. M., & Páscoa, R. N. M. J. (2023). Authentication/discrimination, identification and quantification of cinnamon adulterants using NIR spectroscopy and different chemometric tools: A tutorial to deal with counterfeit samples. *Food Control, 147*, 109619. https://doi.org/10.1016/j.foodcont.2023.109619
12. Cruz-Tirado, J. P., Brasil, Y. L., Lima, A. F., Pretel, H. A., Godoy, H. T., Barbin, D., & Siche, R. (2023). Rapid and non-destructive cinnamon authentication by NIR-hyperspectral imaging and classification chemometrics tools. *Spectrochimica Acta Part A: Molecular and Biomolecular Spectroscopy*, *289*, 122226. https://doi.org/10.1016/j.saa.2022.122226
13. Dashti, A., Weesepoel, Y., Müller-Maatsch, J., Parastar, H., Kobarfard, F., Daraei, B., & Yazdanpanah, H. (2022). Assessment of meat authenticity using portable Fourier transform infrared spectroscopy combined with multivariate classification techniques. *Microchemical Journal*, *181*, 107735. https://doi.org/10.1016/j.microc.2022.107735
14. Dave, G., & Modi, H. (2018). FT-IR method for estimation of phytic acid content during bread-making process. *Journal of Food Measurement and Characterization*, *12*, 2202-2208. https://doi.org/10.1007/s11694-018-9836-y
15. De Angelis, D., Summo, C., Pasqualone, A., Faccia, M., & Squeo, G. (2024). Advancements in food authentication using soft independent modelling of class analogy (SIMCA): a review. *Food Quality and Safety, 8*. https://doi.org/10.1093/fqsafe/fyae032
16. de Lima, A. B. S., Batista, A. S., de Jesus, J. C., de Jesus Silva, J., de Araújo, A. C. M., & Santos, L. S. (2020). Fast quantitative detection of black pepper and cumin adulterations by near-infrared spectroscopy and multivariate modeling. *Food Control, 107*, 106802. https://doi.org/10.1016/j.foodcont.2019.106802
17. Dimitriou, L., Koureas, M., Kapageridou, S., Pappas, C. S., Manouras, A., & Malissiova, E. (2025). Meat authenticity predictive classification by implementing Fourier transform infrared spectroscopy (FTIR) combined with chemometrics. *Journal of Food Composition and Analysis, 145*, 107862. https://doi.org/10.1016/j.jfca.2025.107862
18. Fattahi, S. H., & Seyfari, A. K. Y. (2025). Accurate detection of safflower adulteration in saffron by ATR-FTIR spectroscopy and feature selection and machine learning algorithms: SH Fattahi and AKY Seyfari. *Journal of Food Measurement and Characterization, 19*, 6295-6309. https://doi.org/10.1007/s11694-025-03371-x
19. Feltes, G., Ballen, S. C., Steffens, J., Paroul, N., & Steffens, C. (2023). Differentiating True and False Cinnamon: Exploring Multiple Approaches for Discrimination. *Micromachines, 14*(10), 1819. https://doi.org/10.3390/mi14101819
20. Fiorino, G. M., Garino, C., Arlorio, M., Logrieco, A. F., Losito, I., & Monaci, L. (2018). Overview on untargeted methods to combat food frauds: a focus on fishery products. *Journal of Food Quality, 2018*, 1581746. https://doi.org/10.1155/2018/1581746
21. Galvin-King, P. (2020). *The detection of economically motivated adulteration in the herb and spice industry* (Doctoral thesis, Queen's University Belfast). Belfast, Northern Ireland: Queen's University Belfast.
22. Goel, B., & Mishra, S. (2020). Medicinal and nutritional perspective of cinnamon: A mini-

review. *European Journal of Medicinal Plants*, *31*(3), 10-16. https://doi.org/10.9734/EJMP/2020/v31i330218

23. Greenacre, M., Groenen, P. J. F., Hastie, T., d'Enza, A. I., Markos, A., & Tuzhilina, E. (2022). Principal component analysis. *Nature Reviews Methods Primers*, *2*, 100. https://doi.org/10.1038/s43586-022-00184-w
24. Hajiseyedrazi, Z. S., Khorrami, M. K., & Mohammadi, M. (2024). Alternating conditional expectation (ACE) algorithm and supervised classification models for rapid determination and classification of the adulterated cinnamon samples using diffuse reflectance FT-IR spectroscopy. *Journal of Food Composition and Analysis*, *131*, 106226. https://doi.org/10.1016/j.jfca.2024.106226
25. Hashemi-Nasab, F. S., Talebian, S., & Parastar, H. (2023). Multiple adulterants detection in turmeric powder using Vis-SWNIR hyperspectral imaging followed by multivariate curve resolution and classification techniques. *Microchemical Journal*, *185*, 108203. https://doi.org/10.1016/j.microc.2022.108203
26. Hu, J., Zhang, Y., Xiao, Z., & Wang, X. (2018). Preparation and properties of cinnamon-thyme-ginger composite essential oil nanocapsules. *Industrial Crops and Products*, *122*, 85-92. https://doi.org/10.1016/j.indcrop.2018.05.058
27. Huang, Z., Pang, D., Liao, S., Zou, Y., Zhou, P., Li, E., & Wang, W. (2021). Synergistic effects of cinnamaldehyde and cinnamic acid in cinnamon essential oil against S. pullorum. *Industrial Crops and Products*, *162*, 113296. https://doi.org/10.1016/j.indcrop.2021.113296
28. Jahan, R. A., & Uddin, N. (2024). FT-IR analyses in food authentication: Food safety and quality assurance. In M. Kuddus, S. A. Ashraf, & P. Rahman (Eds.), *Food safety: Quality control and management* (pp. 52–67). Boca Raton, FL: CRC Press. https://doi.org/10.1201/9781003334859-4
29. Jiménez-Carvelo, A. M., Tonolini, M., McAleer, O., Cuadros-Rodríguez, L., Granato, D., & Koidis, A. (2021). Multivariate approach for the authentication of vanilla using infrared and Raman spectroscopy. *Food Research International*, *141*, 110196. https://doi.org/10.1016/j.foodres.2021.110196
30. Kaavya, R., Pandiselvam, R., Mohammed, M., Dakshayani, R., Kothakota, A., Ramesh, S. V, Cozzolino, D., & Ashokkumar, C. (2020). Application of infrared spectroscopy techniques for the assessment of quality and safety in spices: a review. *Applied Spectroscopy Reviews*, *55*(7), 593-611. https://doi.org/10.1080/05704928.2020.1713801
31. Khanban, F., Garmarudi, A. B., Parastar, H., & Toth, G. (2022). Evaluation of FT-IR spectroscopy combined with SIMCA and PLS-DA for detection of adulterants in pistachio butter. *Infrared Physics & Technology*, *127*, 104369. https://doi.org/10.1016/j.infrared.2022.104369
32. Khodabakhshian, R., & Abbaspour-Fard, M. H. (2020). Pattern recognition-based Raman spectroscopy for non-destructive detection of pomegranates during maturity. *Spectrochimica Acta Part A: Molecular and Biomolecular Spectroscopy*, *231*, 118127. https://doi.org/10.1016/j.saa.2020.118127
33. Khodabakhshian, R., Bayati, M. R., & Emadi, B. (2021). An evaluation of IR spectroscopy for authentication of adulterated turmeric powder using pattern recognition. *Food Chemistry*, *364*, 130406. https://doi.org/10.1016/j.foodchem.2021.130406
34. Khodabakhshian, R., Lavasani, H. S., & Weller, P. (2023). A methodological approach to preprocessing FTIR spectra of adulterated sesame oil. *Food Chemistry*, *419*, 136055. https://doi.org/10.1016/j.foodchem.2023.136055
35. Lixourgioti, P., Goggin, K. A., Zhao, X., Murphy, D. J., van Ruth, S., & Koidis, A. (2022). Authentication of cinnamon spice samples using FT-IR spectroscopy and chemometric classification. *LWT*, *154*, 112760. https://doi.org/10.1016/j.lwt.2021.112760

36. Lopes, J. D. S., de Lima, A. B. S., da Cruz Cangussu, R. R., da Silva, M. V., Ferrão, S. P. B., & Santos, L. S. (2022). Application of spectroscopic techniques and chemometric methods to differentiate between true cinnamon and false cinnamon. *Food Chemistry*, *368*, 130746. https://doi.org/10.1016/j.foodchem.2021.130746
37. Montgomery, H., Haughey, S. A., & Elliott, C. T. (2020). Recent food safety and fraud issues within the dairy supply chain (2015–2019). *Global Food Security*, *26*, 100447. https://doi.org/10.1016/j.gfs.2020.100447
38. Moreno, E. K. G., de Macêdo, I. Y. L., Batista, E. A., Machado, F. B., Santos, G. R., Andrade, D. M. L., Rocha, M. L., Lima, N. M., Vaz, B. G., & Gil, E. S. (2022). Evaluation of antioxidant potential of commercial cinnamon samples and its vasculature effects. *Oxidative Medicine and Cellular Longevity*, *2022*, 1992039. https://doi.org/10.1155/2022/1992039
39. Nargesi, M. H., Amiriparian, J., Bagherpour, H., & Kheiralipour, K. (2024). Detection of different adulteration in cinnamon powder using hyperspectral imaging and artificial neural network method. *Results in Chemistry*, *9*, 101644. https://doi.org/10.1016/j.rechem.2024.101644
40. Nicolaou, N., Xu, Y., & Goodacre, R. (2010). Fourier transform infrared spectroscopy and multivariate analysis for the detection and quantification of different milk species. *Journal of Dairy Science*, *93*(12), 5651-5660. https://doi.org/10.3168/jds.2010-3619
41. Nicolau, S. T., & Matzger, A. J. (2024). An evaluation of resolution, accuracy, and precision in FT-IR spectroscopy. *Spectrochimica Acta Part A: Molecular and Biomolecular Spectroscopy*, *319*, 124545. https://doi.org/10.1016/j.saa.2024.124545
42. Omuya, E. O., Okeyo, G. O., & Kimwele, M. W. (2021). Feature selection for classification using principal component analysis and information gain. *Expert Systems with Applications*, *174*, 114765. https://doi.org/10.1016/j.eswa.2021.114765
43. Özçimen, D., & Ersoy-Meriçboyu, A. (2010). Adsorption of copper (II) ions onto hazelnut shell and apricot stone activated carbons. *Adsorption Science & Technology*, *28*, 327-340. https://doi.org/10.1260/0263-6174.28.4
44. Pages-Rebull, J., Pérez-Ràfols, C., Serrano, N., & Díaz-Cruz, J. M. (2024). Analytical methods for cinnamon authentication. *Trends in Food Science & Technology*, *146*, 104388. https://doi.org/10.1016/j.tifs.2024.104388
45. Pagliari, S., Forcella, M., Lonati, E., Sacco, G., Romaniello, F., Rovellini, P., Fusi, P., Palestini, P., Campone, L., & Labra, M. (2023). Antioxidant and anti-inflammatory effect of cinnamon (*Cinnamomum verum* J. Presl) bark extract after in vitro digestion simulation. *Foods*, *12*, 452. https://doi.org/10.3390/foods12030452
46. Querido, W., Kandel, S., & Pleshko, N. (2021). Applications of vibrational spectroscopy for analysis of connective tissues. *Molecules*, *26*, 922. https://doi.org/10.3390/molecules26040922
47. Rana, P., Liaw, S. Y., Lee, M. S., & Sheu, S. C. (2021). Discrimination of four Cinnamomum species with physico-functional properties and chemometric techniques: application of PCA and MDA models. *Foods*, *10*, 2871. https://doi.org/10.3390/foods10112871
48. RP, S., Sankar, M., Sukumaran, R. K., & Savithri, S. (2024). Rapid estimation of the chemical composition of rice straw using FTIR spectroscopy: A chemometric investigation. *Biomass Conversion and Biorefinery*, *14*, 11829-11847. https://doi.org/10.1007/s13399-022-03508-8
49. Shawky, E., Nahar, L., Nassief, S. M., Sarker, S. D., & Ibrahim, R. S. (2024). Spice Authentication by Near-Infrared Spectroscopy: Current Advances, Limitations, and Future Perspectives. *Trends in Food Science & Technology*, 104522. https://doi.org/10.1016/j.tifs.2024.104522
50. Spence, C. (2023). Cinnamon: The historic spice, medicinal uses, and flavour chemistry. *International Journal of Gastronomy and Food Science*, *35*, 100858. https://doi.org/10.1016/j.ijgfs.2023.100858

51. Sudarsh, S., & Müller-Maatsch, J. (2023). Evaluation of on-site testing methods with a novel 3-in-1 miniaturized spectroscopic device for cinnamon screening. *Talanta, 256*, 124195. https://doi.org/10.1016/j.talanta.2022.124195
52. Suriyagoda, L., Mohotti, A. J., Vidanarachchi, J. K., Kodithuwakku, S. P., Chathurika, M., Bandaranayake, P. C. G., Hetherington, A. M., & Beneragama, C. K. (2021). "Ceylon cinnamon": Much more than just a spice. *Plants, People, Planet* 3, 319-336. https://doi.org/10.1002/ppp3.10192
53. Velázquez, R., Rodríguez, A., Hernández, A., Casquete, R., Benito, M. J., & Martín, A. (2023). Spice and Herb Frauds: Types, Incidence, and Detection: The State of the Art. *Foods, 12*, 3373. https://doi.org/10.3390/foods12183373
54. Vinothkanna, A., Dar, O. I., Liu, Z., & Jia, A. Q. (2024). Advanced detection tools in food fraud: A systematic review for holistic and rational detection method based on research and patents. *Food Chemistry*, 138893. https://doi.org/10.1016/j.foodchem.2024.138893
55. Wang, Y., Han, M., Xu, Y., Wang, X., Cheng, M., Cui, Y., Xiao, Z., & Qu, J. (2023). Effect of potato peel on the determination of soluble solid content by visible near-infrared spectroscopy and model optimization. *Analytical Methods, 15*, 3854-3862. https://doi.org/10.1039/d3ay00774j
56. Wu, Q., Mousa, M. A. A., Al-Qurashi, A. D., Ibrahim, O. H. M., Abo-Elyousr, K. A. M., Rausch, K., Aal, A. M. K. A., & Kamruzzaman, M. (2023). Global calibration for non-targeted fraud detection in quinoa flour using portable hyperspectral imaging and chemometrics. *Current Research in Food Science, 6*, 100483. https://doi.org/10.1016/j.crfs.2023.100483
57. Wu, Y., Xian, Y., Guo, X., Chen, L., Zhao, X., Wang, B., & Wang, L. (2018). Development and validation of a screening and quantification method for simultaneous determination of seven fluorescent whitening agents in commercial flour using UPLC–MS/MS. *Food Chemistry, 243*, 162-167. https://doi.org/10.1016/j.foodchem.2017.09.110
58. Yadav, A., Nimi, C., Kapoor, M., & Singh, R. (2025). A quick and non-destructive approach to combat timber adulteration using attenuated total reflectance Fourier transform infrared spectroscopy and chemometrics. *The Science of Nature, 112*, 21. https://doi.org/10.1007/s00114-025-01970-8
59. Yasmin, J., Ahmed, M. R., Lohumi, S., Wakholi, C., Lee, H., Mo, C., & Cho, B. K. (2019). Rapid authentication measurement of cinnamon powder using FT-NIR and FT-IR spectroscopic techniques. *Quality Assurance and Safety of Crops & Foods, 11*(3), 257-267. https://doi.org/10.3920/QAS2018.1318
60. Zhang, Z., Zhao, Y., Chen, X., Li, Wei, Li, Wen, Du, J., & Wang, L. (2022). Effects of cinnamon essential oil on oxidative damage and outer membrane protein genes of Salmonella enteritidis cells. *Foods, 11*(15), 2234. https://doi.org/10.3390/foods11152234

کاربرد طیف‌سنجی مادون‌قرمز تبدیل فوریه و روش‌های طبقه‌بندی کمومتریکس در شناسایی تقلبات پودر دارچین

محمد مسعودی[۱]، رسول خدابخشیان کارگر[۱*]، محمودرضا گلزاریان[۱]

تاریخ دریافت: ۱۴۰۵/۰۲/۱۵
تاریخ پذیرش: ۱۴۰۵/۰۴/۲۷

چکیده

دارچین یک ادویه معطر با ارزش بالا است که به‌طور گسترده در صنایع غذایی و دارویی مورد استفاده قرار می‌گیرد. به دلیل کاربردهای گسترده، دارچین در معرض تقلب غذایی قرار دارد که وجود روش‌های معتبر تشخیص اصالت را ضروری می‌سازد. این مطالعه از طیف‌سنجی فروسرخ تبدیل فوریه (FTIR) و تحلیل الگوهای طیفی به‌منظور ایجاد یک روش قابل‌اطمینان برای تشخیص تقلب در پودر دارچین، با مقایسه نمونه‌های اصیل و نمونه‌های دستکاری‌شده، استفاده می‌کند. هدف نهایی، ارائه‌ی یک روش‌شناسی عملی برای شناسایی تقلب در صنعت ادویه است. در این کار، از طیف‌سنجی فروسرخ تبدیل فوریه (FTIR) به همراه تکنیک‌های تشخیص الگو برای احراز اصالت پودر دارچین استفاده شد. به‌منظور شناسایی و طبقه‌بندی نمونه‌های تقلبی (با مواد افزودنی شامل: پودر سویا، پودر پوست فندق و پودر نان خشک، در غلظت‌های مختلف ۵، ۱۰ و ۱۵ درصد وزنی/وزنی) به‌صورت غیرمخرب، از تحلیل مؤلفه‌های اصلی (PCA) به‌عنوان روش بدون نظارت و از تحلیل تفکیکی حداقل مربعات جزئی (PLS-DA) و مدل‌سازی مستقل نرمال مشابهت رده‌ها (SIMCA) به‌عنوان رویکردهای تشخیص الگوی نظارت‌شده استفاده شد. نتایج نشان داد که اگرچه داده‌های طیفی نمونه‌ها با استفاده از تکنیک PCA به‌خوبی طبقه‌بندی شدند، اما هم‌پوشانی‌هایی بین برخی گروه‌ها مشاهده گردید. دقت کلی طبقه‌بندی توسط طبقه‌بندهای SIMCA و PLS-DA به‌ترتیب ۸۳ و ۹۰ درصد بود. بر اساس مدل سازی PCA، روش SIMCA امکان طبقه‌بندی نمونه‌ها را به دو گروه مجزا (خالص در برابر تقلبی) فراهم کرد و دقت طبقه‌بندی این مدل دوکلاسی به ۱۰۰ درصد رسید. این یافته‌ها کارایی ترکیب طیف‌سنجی FTIR با تکنیک‌های تشخیص الگو را برای احراز اصالت غیرمخرب و مقاوم پودر دارچین تقلبی تأیید کرده و به کنترل کیفیت در صنعت ادویه کمک می‌نماید.

واژه‌های کلیدی: تشخیص تقلب، دارچین، طیف‌سنجی مادون قرمز، کنترل کیفیت

۱- گروه مهندسی بیوسیستم، دانشکده کشاورزی، دانشگاه فردوسی مشهد، مشهد، ایران
(*- نویسنده مسئول: Email: Khodabakhshian@um.ac.ir)

https://doi.org/10.22067/jam.2026.98580.1489